BNL-209422-2018-JAAM

Phase transitions of alpha-quartz at elevated temperatures under dynamic compression using a membrane-driven diamond anvil cell: Clues to impact cratering?

E. Carl, L. Ehm

To be published in "METEORITICS & PLANETARY SCIENCE"

August 2018

Photon Sciences

Brookhaven National Laboratory

U.S. Department of Energy

USDOE Office of Science (SC), Basic Energy Sciences (BES) (SC-22)

DISCLAIMER

Phase transitions of α-quartz at elevated temperatures under dynamic compression using a membrane-driven diamond anvil cell: Clues to impact cratering?

Eva-Regine CARL [a,e*], Hanns-Peter LIERMANN [b], Lars EHM [c,d], Andreas DANILEWSKY [e], and Thomas KENKMANN [a]

[a] Institut für Geo- und Umweltnaturwissenschaften, Geologie, Albertstr. 23b, Albert-Ludwigs-Universität, 79104 Freiburg, Germany
[b] DESY, Notkestraße 85, 22607 Hamburg, Germany
[c] Stony Brook University, Mineral Physics Institute, Stony Brook, NY 11794-2100, USA
[d] National Synchrotron Light Source II, Brookhaven National Laboratory, Upton, NY 11973-500, USA
[e] Institut für Geo- und Umweltnaturwissenschaften, Kristallographie, Hermann-Herder-Str. 5, Albert-Ludwigs-Universität, 79104 Freiburg, Germany

*Corresponding author. E-mail: eva-reginecarl@gmx.net

Keywords: quartz, X-ray diffraction, high pressure, high temperature

Abstract

Coesite and stishovite are high-pressure silica polymorphs known to have been formed at several terrestrial impact structures. They have been used to assess pressure and temperature conditions that deviate from equilibrium formation conditions. Here we investigate the effects of non-hydrostatic, dynamic stresses on the formation of high-pressure polymorphs and the amorphization of α-quartz at elevated temperatures. The obtained disequilibrium states are compared with those predicted by phase diagrams derived from static experiments under equilibrium conditions. We create dynamic conditions utilizing a membrane-driven diamond anvil cell and study the phase transformations in α-quartz *in situ* by synchrotron powder x-ray diffraction. Phase transitions of α-quartz are studied up to 77.2 GPa and temperatures of 1160 K at compression rates ranging between 0.10 and 0.37 GPa/s. Coesite starts forming above 760 K in the pressure range between 2 and 11 GPa. At 1000 K coesite starts to transform into stishovite. This phase transition is not completed at 1160 K in the same pressure range. Therefore, the temperature initiates the phase transition from α-quartz to coesite, and the transition from coesite to stishovite. Below 1000 K and during compression, α-quartz becomes amorphous and partially converts to stishovite. This phase transition occurs between 25 and 35 GPa. Above 1000 K, no amorphization of α-quartz is observed. High temperature experiments reveal the strong thermal dependence of the formation of coesite and stishovite under non-hydrostatic and disequilibrium conditions.

1. Introduction

α-Quartz is one of the most abundant minerals in the Earth's crust and has been studied extensively under equilibrium conditions. Its wide occurrence including many shock effects makes it the most widely used shock barometer (Stöffler and Langenhorst 1994; French and Koeberl 2010) in impact studies. High-pressure phases of SiO_2, namely coesite and stishovite, form under quasi-static as well as under highly dynamic conditions. Coesite, for instance, was reported from ultra-high pressure metamorphic zones (e.g., Chopin 1984), kimberlites (Smyth and Hatton 1977), and is known from several impact sides such as the Ries (Chao et al. 1960; ElGoresy et al. 2001) or the Wabar craters (Chao et al. 1961). Knowledge of the high-pressure structural stability of SiO_2 and the underlying mechanisms under dynamic conditions can improve the understanding of phase transitions, geological processes in the Earth's interior, glass formation and chemical bonding.

The thermodynamic stability fields of high pressure polymorphs of α-quartz have been experimentally and theoretically investigated since 1953 (Coes 1953) under quasi-hydrostatic conditions in equilibrium: At room temperature, α-quartz transforms to coesite with four-fold coordinated Si at 2 GPa and to stishovite with six-fold coordinated Si (Stishov et al. 1961) at 8 GPa (Kirfel et al. 2001).

Under dynamic and non-hydrostatic conditions, its phase diagram becomes intricate and exhibits many different crystalline phases. Due to the relatively strong Si-O bonding, compression of α-quartz without sufficient heating results in formation of complex metastable phases, featuring partially silicon in six-fold coordination (e.g., Choudhury et al. 2006 and Carl et al. 2017).

Under dynamic compression, α-quartz undergoes a pressure-induced amorphization in the pressure range 18-35 GPa (McNeil et al. 1992; Kingma et al. 1993a; Kingma et al. 1993b). Furthermore, theoretical investigations of the SiO_2 system predict a number of competing metastable post-quartz phases that precede or coexist along with amorphization (Choudhury et al. 2006; Teter et al. 1998; Wentzcovitch et al. 1998). The structural transformation pathways are highly dependent on the precursor phase and, beside the hydrostatic pressure, the deviatoric component of the stress tensor is important (Ohtaka et al. 2001; Huang et al. 2006; Haines et al. 2000).

α-Quartz ($P3_221$ space group) may transform to a monoclinic ($P2_1/c$ space group) post-quartz phase (Haines et al. 2001) between 20-25 GPa. Its structure is built of 3 x 2 kinked chains of edge-sharing SiO_6-octahedra. Theoretical calculations by Teter et al. (1998) and Martoňák et al. (2007) reveal that this phase transformation is diffusionless. This phase is closely related to stishovite ($P4_2/mnm$ space group) that is built of edge-sharing octahedra forming straight chains. These two structures are competing because of very similar activation energies (Teter et al. 1998). The monoclinic post-quartz phase has not been discovered in natural geological settings.

Studying the structure and the formation of these phases is experimentally challenging due to sluggish transitions, enhanced metastability regions and formation of poorly crystallized materials. Such conditions usually cause weak X-ray diffraction patterns that are difficult to interpret, often resulting in contradictory interpretations. Due to this great complexity, previous investigations of SiO_2 at high pressure and temperature have left many unanswered questions concerning the behavior of the material.

A recently published study reveals that α-quartz partially transforms directly to stishovite during non-hydrostatic compression at room temperature, bypassing the stability field of coesite (Carl et al. 2017). While the phase transition occurs between 18 and 38 GPa, most of the sample becomes amorphous. Furthermore, diffraction peaks of the monoclinic post-quartz phase occur prior to the transition to stishovite.

Our time-resolved X-ray diffraction experiments under dynamic compression provide insights into the kinetics of high-pressure phase transitions of α-quartz, making use of fast data acquisition now available at synchrotron sources. Building on the findings of Carl et al. (2017) this study is devoted to address the effect of temperature on the occurrence of SiO_2-high-pressure phases under dynamic deformation conditions.

While loading and unloading rates are orders of magnitude too small to compare them to shock loading, it provides information on the transformation kinetics of SiO_2 high-pressure polymorphs coesite and stishovite under non-hydrostatic and dynamic conditions.

2. Experimental setup

The experiments were conducted utilizing a membrane-driven four-pin diamond anvil cell (4pDAC), which was equipped with diamonds of a culet size of 0.3 mm. The culets indented 0.25 mm Re-gaskets to 0.036 – 0.042 mm thickness. For the experiments denoted as *SiO2_heat_01*, *_02* and *_03*, a 0.1 mm hole was drilled as a sample chamber. For the experiments *SiO2_heat_04*, *_05* and *_06*, a 0.3 mm hole was drilled to install an amorphous B-gasket of a thickness of 0.05 mm. The amorphous B-gasket featured a 0.08 mm sample chamber at its center. In general, ceramic gaskets such as amorphous Boron inserts are more stable and prevented shearing of the gasket (as common in metal gaskets) as well as a strong shift of the gasket during heating. A mixture of α-quartz powder (Alfa Aesar, 99.5%, -400 Mesh, 2 Micron, LOT: L01W019) and Pt (about 8 wt.%) or Au powder (about 10 wt.%) for internal pressure calibration was filled into the gasket hole without a pressure medium. The experiments were conducted at elevated temperatures up to 1160 K (Table 1) using a graphite resistance heater depicted in Fig. 1.

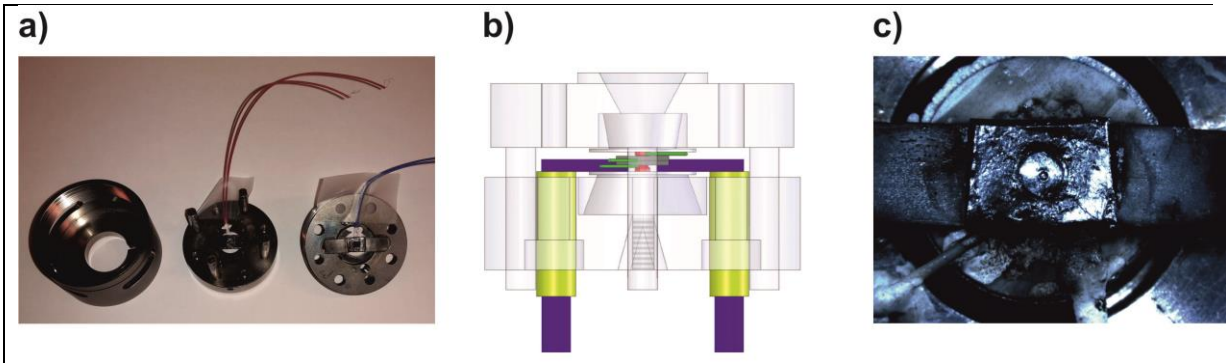

Figure 1: a) Image and b) 3D representation of the assembled graphite resistive heated four pin DAC. c) Image of the 4 pin DAC after the experiment.

Before starting an experiment, the diamonds were forced to touch the gasket by pressing the two halves of the DAC together by inflating the membrane. Then, the sample was heated up to the desired temperature at nearly constant rates between 1 and 3 K/min. The heating caused the pressure to increase. By deflating the membrane, the pressure was slightly decreased during heating but unfortunately not kept constant. At the desired temperature, the sample was compressed through the activation of the membrane pressure controller resulting in a linear increase of pressure. The maximum pressure was kept constant for a certain time and the experiment concluded with decompression.

Monochromatic X-ray powder diffraction experiments were conducted at the Extreme Conditions Beamline (ECB) P02.2 at PETRA III, DESY, Hamburg, Germany (Liermann et al. 2015). In order to achieve an optimal signal-to-noise ratio of the diffraction patterns, the energy of the X-rays was tuned to 25.6 keV and the focus of the X-ray beam was enlarged to 8 (H) x 3 (V) µm² through focusing with Compound Refractive Lens system. The wavelength was 0.4847 Å for experiments *SiO2_heat_01* and *_02* (Table 1) and to 0.4869 Å for experiments *SiO2_heat_03*, *_04*, *_05* and *_06*. The sample to detector distance was calibrated using the CeO_2 standard (NIST 687) and varied between 440.2978 mm (*SiO2_heat_01* and _02) and 424.1328 mm (*SiO2_heat_03*, *_04*, *_05* and *_06*). The exposure time of the diffraction patterns collected during heating was 10 seconds. During compression and decompression, diffraction images were collected every four seconds. They were recorded on a Perkin Elmer area detector (model XRD 1621) and were subsequently converted to one-dimensional diffraction patterns using the software dioptas (Prescher and Prakapenka 2015).

The experimental data were surveyed using the P02 Processing Tool (Konopkova et al. 2015). This software is an online tool to quickly process and plot one-dimensional diffraction patterns as a function of frame number and may be used to create two- and three-dimensional contour plots as function of time. The use of the tool was essential to get a first overview of the compression experiment and to define the onset of phase transitions. For a detailed analysis of the diffraction patterns including the identification of phases and the determination of cell parameters, we used the program package FullProf (Rodríguez-Carvajal 1993).

The LeBail analysis (LeBail et al. 1988) was carried out from 3 to 15° 2θ for all diffraction patterns. For each phase, the lattice parameters and the width of the reflections at half maximum

(FWHM) were refined using the split pseudo-Voigt function. Given that each experiment consists of between 1,500 and 3,690 diffraction patterns, a sequential fitting was carried out, if possible.

After inspection of the X-ray diffraction pattern, four phases were further considered: α-quartz, coesite, stishovite and the monoclinic post-quartz phase. The starting lattice parameters were a = 4.91239 ± 4e-05 Å and c = 5.40385 ± 7e-05 Å for α-quartz (Will et al. 1988), a = 7.1356, b = 12.3692 and c = 7.1736 for coesite (Levien and Prewitt 1981) and a = 4.1773 Å and c = 2.6655 Å for stishovite (Hill et al. 1983). For the monoclinic post-quartz phase, the lattice parameters a = 7.66 Å, b = 4.10Å, c = 5.03 Å and β = 117.9° (Haines et al. 2001) were used. The unit cell dimensions computed from the 111, 200, 220 and 311 diffraction lines of gold or platinum resulted in pressure estimates using a third order Birch-Murnaghan Equation of State (Birch 1951) with the bulk modulus from Anderson et al. (1989) for gold and the bulk modulus from Fei et al. (2007) for platinum.

The parameters of the compression cycle of the six experiments are listed in Table 1. The compression started at P_{start} at rates varying between 0.1 GPa/s to 0.37 GPa/s with increasing temperature of the experiments. The maximum pressure P_{max} after compression ranged between 31.1 GPa (*SiO2_heat_01*) and 77.2 GPa (*SiO2_heat_02*) and was held for up to two hours (Table 1). Decompression did not reach ambient pressures but stopped at P_{min} due to friction on the pins of the 4pDAC.

Table 1: The experimental conditions of the six experiments at elevated temperature.

SiO2_heat_x	Temperature [K]	Compression rate on sample [GPa/s]	P_{start} [GPa]	P_{max} [GPa]	Hold at P_{max} [min]	Decompression rate on sample [GPa/s]	P_{min} [GPa]
01	600	0.14	2.3	31.1	120	0.01	24.6
02	600	0.37	7.9	77.2	10	0.3	39.6
03	640	0.14	0.0001	54.5	10	0.06	31.7
04	880	0.10	10.8	45.3	10	0.20	12.9
05	1100	0.13	8.1	44.0	10	*	*
06	1160	0.34	8.4	51.9	10	0.16	35.9

* Diamonds broke.

During compression, the identification of phases in the experiments was difficult because the non-hydrostatic compression caused high stresses on the sample that result in broadening of the reflections. Moreover, the weak scattering of α-quartz and the strong Compton scattering of the diamonds decreased the signal-to-noise ratio. Consequently, a LeBail-analysis reached the stability of the algorithm and the position of the low intensity reflections could not be determined precisely. They differed strongly from one refinement step to the next or remain at positions where no reflection was observed.

3. Results

Exemplary diffraction patterns collected during heating of the sample *SiO2_heat_06* are illustrated in Figure 2. The heating was constant at a rate of about 2 K/min. Due to the thermal expansion of the cell, the pressure increases which we tried to compensate by defeating the membrane, resulting in pressure drops during the heating rather than a continuing increase. During the heating and compression, two phase transitions are observed:

At 760 K, α-quartz transforms to coesite as indicated by the occurrence of the 040 reflection of coesite, which is the strongest reflection of this phase. This transition is complete at 920 K and coesite remains stable until 1000 K. At this temperature, stishovite starts to form as indicated be the appearance of the 110 reflection of stishovite. The time scale for these phase transitions was between 5 and 15 minutes. The phase transition from coesite to stishovite is not completed at the maximum temperature of 1160 K. During heating, the pressure did not exceed 11 GPa in all experiments.

The diffraction patterns collected during heating also reveal a broadening of the reflections of α-quartz at 570 K, indicating a reduction in crystallite size and/or strain due to the significant increase in non-hydrostatic pressure from 2.8 to 4.4 GPa (Figure 2). Immediately before the transformation to coesite between 730 to 750 K and a pressure around 3 GPa, recrystallization occurs as the width of the reflections decreases again as can be clearly seen with respect to the 100 reflection of α-quartz at 6.8 °2θ in Figure 2. The reflections of coesite and stishovite do not vary in width and/or integrated intensity.

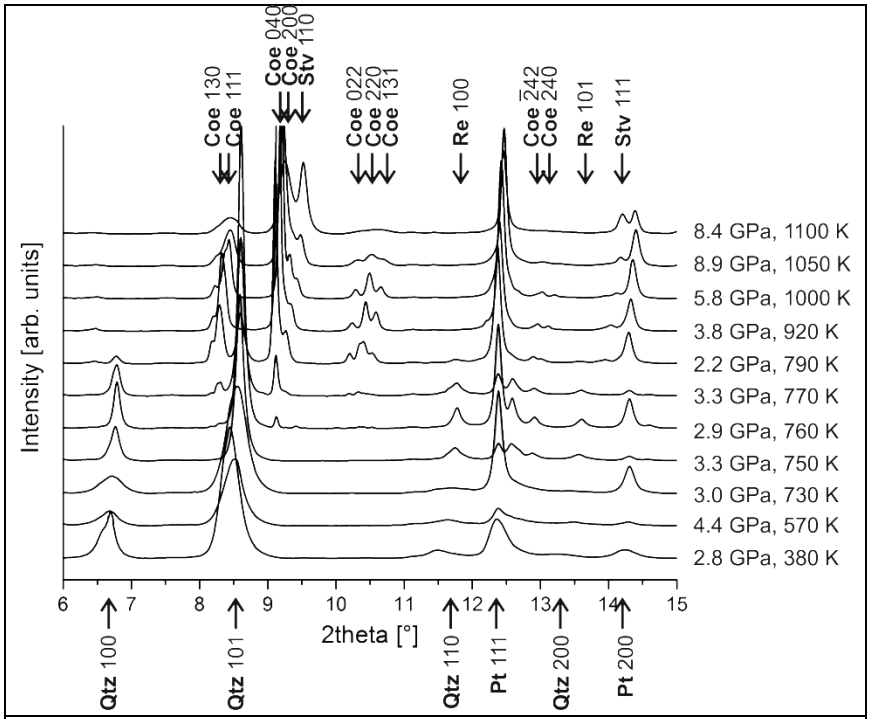

Figure 2: The heating of the sample of experiment *SiO2_heat_06*: At 570 K, the reflections of α-quartz broaden but the width decreases immediately before the phase transition to coesite. At 760 K, α-quartz (Qtz) starts to transform into coesite (Coe). At 920 K, reflections of stishovite (Stv) are observed. There are no variations in width and/or integrated intensity of the reflections of coesite

and stishovite. The pressure increases slightly due to thermal expansion of the cell. The pressure is obtained based on the high temperature and pressure EoS of platinum (Pt).

Figure 3 features the compression cycle of the sample at constant temperatures of 880 K (Figure 3a) and 1100 K (Figure 3b) at similar compression rates. During compression of both experiments, α-quartz transforms to stishovite at pressures between 25 and 35 GPa and remains stable to maximum pressure. At 880 K, furthermore, most of the sample becomes amorphous (Figure 3a) as indicated by the broadening as well as a strong decrease in the integrated intensity of the reflections. The amorphization starts at 16 GPa and progresses with continuing compression until α-quartz transforms into stishovite. The amount of stishovite formed is very small and its long-range order decreases as shown by the weak and broad reflections of this phase. After the phase transition, amorphization only progresses minimal as indicated by diffraction patterns taken at maximum pressures between 31.1 GPa and 77.2 GPa. At maximum pressures, reflections of the monoclinic post-quartz phase were also observed in diffraction patterns collected over 60 seconds. Considering the recent study of Carl et al. (2017), the reflections of the monoclinic post-quartz phase might occur around 10 GPa during compression. Above 1000 K, however, the experiments show no amorphization of the sample during compression because a decrease in the integrated intensity of the reflections cannot be observed (Figure 3b). The removal of the background of *SiO2_heat_05* was very challenging. The elevations at 8.6 °2θ and between 11 and 12.2 °2θ in the diffraction patterns in Figure 3b are contributions from the remaining background.

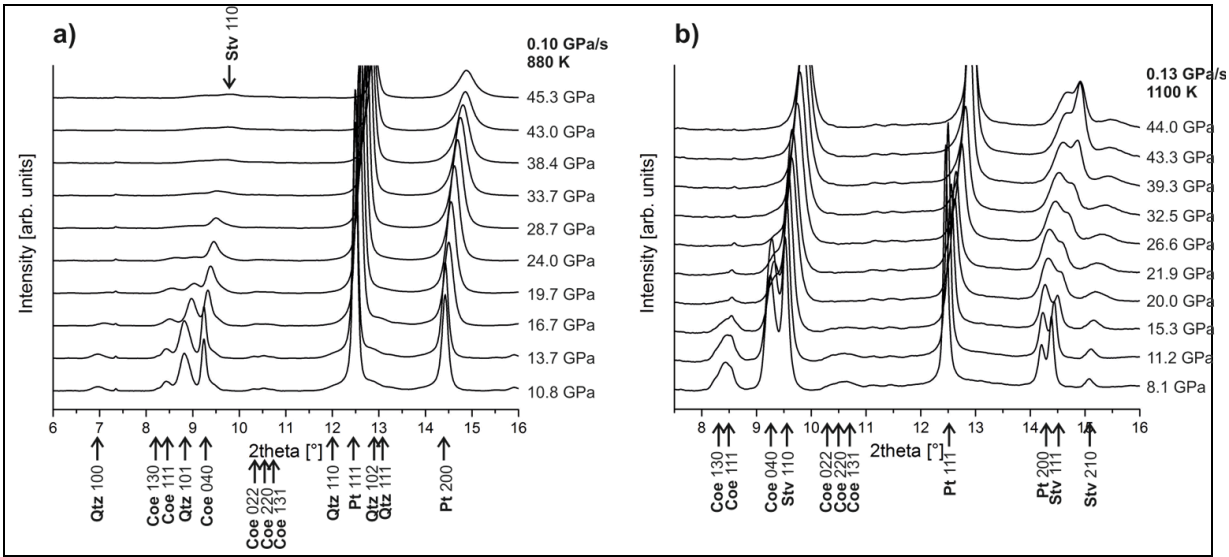

Figure 3: The compression cycle (a) at 880 K and (b) 1100 K. (a) *SiO2_heat_04*: During compression, coesite (Coe) transforms into stishovite (Stv). Along this transition, most of the sample becomes amorphous. (b) *SiO2_heat_05*: During compression, coesite transforms to stishovite. There is no amorphization observed. The pressure is obtained with respect to platinum (Pt).

Figure 4 summarizes the observed phase transitions in the experiments. The black arrows help to follow the temperature-pressure path of the individual experiments. At 760 K and up to 11 GPa, α-quartz starts to transform into coesite. Coesite is stable between 900 K and 1000 K in the pressure range from 2 to 11 GPa. After 1000 K, the transition to stishovite begins but is incomplete at 1160 K. Both phase boundaries feature positive dP/dT slopes as given in literature (Swany et al. 1994; Zhang et al. 1996). Other high temperature phases such as β-quartz or tridymite are not observed. During compression, stishovite forms from α-quartz below 900 K or coesite above 900 K. The experiments indicate strongly varying formation pressures for stishovite ranging between 21 and 38 GPa, making it very difficult to obtain precise phase boundaries. Above 25 GPa, stishovite is stable throughout the entire temperature range from room temperature to 1160 K. Below 1000 K and above 25 GPa, most of the sample is amorphous with only a small fraction of the sample transformed to stishovite. Below 700 K and during compression, α-quartz transforms directly into stishovite, skipping the stability field of coesite.

Stishovite remains stable upon reaching maximum pressure and for the duration of the highest pressure and temperature conditions. During decompression, stishovite reflections remain observable, while no reflections of α-quartz or coesite appear in the patterns.

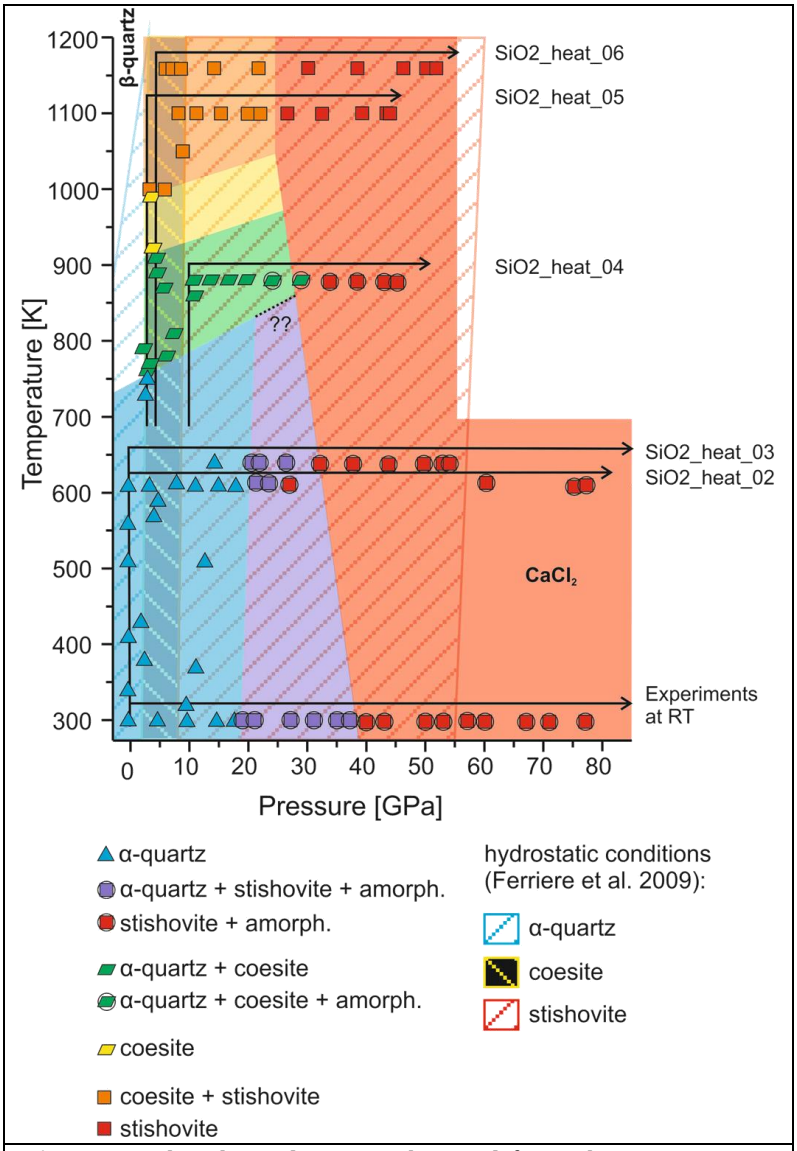

Figure 4: The phase diagram obtained from the experiments *SiO2_heat_01* to *SiO2_heat_06*: Between 2 and 10 GPa, α-quartz transforms to coesite at 760 K. Within the same pressure range, coesite begins to transform to stishovite at 1000 K. During compression, stishovite is formed at various temperatures and remains stable to maximum pressure. The phase boundaries under hydrostatic conditions are added with respect to Ferriere et al. (2009).

4. Discussion

The presented compression experiments on α-quartz provide information on the transformation kinetics of SiO_2 high-pressure polymorphs coesite and stishovite under dynamic conditions. At 760 K and 2-11 GPa, the transformation to coesite begins with the occurrence of the 040 reflection. The transition from α-quartz is completed at 900 K and 2-11 GPa. Coesite remains stable until the onset of the phase transition to stishovite at 1000 K in the pressure range from

2-11 GPa. At the maximum temperature in our experiments, reflections of both coesite and stishovite are observed indicating that the transition is incomplete. These temperature ranges, at which coesite and stishovite are stable, are in agreement with earlier quenching or in situ X-ray diffraction studies. Latter show that α-quartz transforms to coesite between 620 and 1300 K (e.g., Bohlen and Boettcher 1982; Perrilat et al. 2003; Zinn et al. 1995), while coesite transforms to stishovite between 800 K and 1500 K (e.g., Yagi and Akimoto 1976; Zhang et al. 1995). However, these studies report a narrow pressure range for the phase transitions: Coesite forms at around 2 GPa, while stishovite forms in the pressure range between 9 and 11.4 GPa. In our experiments phase transitions to coesite and stishovite take place in the pressure range from 2 to 11 GPa depending on the temperature, i.e. at lower temperatures (< 650 K) only α-quartz is stable, while at higher temperatures first coesite appears and at even higher temperatures a mixture of coesite and stishovite is stable. Only above compression to 25-30 GPa, independent on the temperature, pure stishovite is present. Considering this major variation in transition pressure, it seems that the transitions to high-pressure polymorphs are mostly driven by temperature and thus an expression of the sluggish kinetics of the α-quartz-coesite transition, while pressure under non-hydrostatic conditions does not seem to influence the transformations as strongly. At the same time, the effect of different loading rate explored in the membrane driven DAC on the onset of phase transformations is subordinate (Carl et al. 2017).

The recent fast compression studies on α-quartz reveal that coesite does not form at room temperature and under non-hydrostatic conditions (Carl et al. 2017). The data presented here reveal that the formation of coesite requires elevated temperatures above 760 K and little compression of a few Gigapascal. Coesite remains stable in a temperature window of 400 K and mixed with stishovite up to 1160 K. Stishovite starts to form above 1000 K at low pressures and is the only stable phase above 20-25 GPa and up to 1160 K.

Our experiments reveal that the samples become amorphous below 1000 K during compression. The pressure-induced amorphization of α-quartz starts at 10 GPa at room temperature (Carl et al. 2016) and continues to increase to 16 GPa at 880 K. Both pressures for the start of the amorphization are below the values of 18 GPa to 35 GPa stated in earlier studies (McNeil et al. 1992; Kingma et al. 1993a; Kingma et al. 1993b). We suggest that increased strains in a non-hydrostatic compressed sample result in amorphization at lower pressures, especially when considering that McNeil et al. (1992) and Kingma et al. (1993a) used pressure-transmitting media for their experiments. Above 1000 K, the heating seems to be sufficiently high to allow the formation of the high-pressure phase stishovite without amorphization of the material. However, the transition to stishovite is already starting before the onset of compression phase in this temperature range. Therefore, the added pressure might only help to complete the transition from coesite to stishovite. If the pressure was released, only coesite would be stable.

Along with the amorphization process of α-quartz, the diffraction patterns also feature reflections of the monoclinic post-quartz phase (see also Carl et al. 2017). If the sample does not get amorphous, no reflections of the monoclinic post-quartz phase are observed, indicating a correlation between the amorphization and the occurrence of the monoclinic post-quartz phase. Thus, it is conceivable that the monoclinic post-quartz phase resembles a side product

of the amorphization process, representing a strong disordering of the structure preventing the formation of stishovite due to high amount of amorphous material.

Stishovite remains metastable to the minimum pressure during unloading in all experiment. There is no back-transition to coesite or α-quartz. According to Zhang et al. (1995), the transition from coesite to stishovite is only reversible above 1300 K, which is well above the temperature range of our experiments.

5. Conclusions

We use a combination of a membrane-driven diamond anvil cell and *in-situ* powder x-ray diffraction to study phase transitions of α-quartz at pressures up to 77.2 GPa and 1160 K at compression rates ranging between 0.10 and 0.37 GPa/s. The collection time of one diffraction pattern is as low as four seconds.

Below 760 K, α-quartz transforms directly to stishovite during compression, bypassing the stability field of coesite. This phase transition occurs in our experiments between 25 GPa and 35 GPa. Stishovite remains stable upon reaching maximum pressure and while maintaining maximum pressure. During decompression, stishovite reflections remain observable in absence of α-quartz or coesite. In this temperature range, below 760 K, the transition of stishovite is accompanied by the amorphization of the material starting at about 16 GPa during compression. The material becomes more and more amorphous with proceeding compression until α-quartz transforms to stishovite. The amount of stishovite formed is very small and its long-range order decreases as shown by the weak and broad reflections of this phase. After the phase transition, amorphization progresses only slightly as revealed by diffraction patterns taken at maximum pressures between 31.1 GPa and 77.2 GPa. There are no other changes with respect to the phases of silica observed in these diffraction patterns.

Furthermore, new reflections can be observed up to 25 GPa, which can be assigned to the monoclinic post-quartz phase in the course of compression. These new reflections remain detectable until the maximum pressure is reached. The reflections are not influenced by the phase transition of α-quartz to stishovite. Upon decompression, these reflections do not vanish.

The non-hydrostatic compression experiments reveal the formation of coesite above 760 K in the pressure range between 2 and 11 GPa. With increasing temperature, coesite starts transforming into stishovite at 1000 K in the same pressure range and is incomplete at the highest pressures and temperature explored in this study. Above 1000 K, amorphization of the sample can no longer be observed.

Our dynamic compression experiments provide insights into the kinetics of high-pressure phase transitions of α-quartz: In our experiments, elevated temperatures above 760 K are needed for the formation of coesite at pressures up to 11 GPa. With the obtained phase diagram even suggesting that pressures can be as high as 20 GPa underlining the importance of temperature on the formation of coesite. After compression, stishovite is observed at maximum pressure

throughout the analyzed temperature range. Stishovite is also stable after decompression to minimum pressure between 12.9 and 39.6 GPa.

Although the compression rates in the context of impact cratering are much higher, these in situ investigations of phase transitions are a necessary first step to understand the behavior of SiO_2 under the much faster compression rates of impact events. The latter is envisaged to be studied with a laser shock compressed sample at x-ray free electron lasers (XFELs) in the future.

Acknowledgements

This study was conducted in the framework of the DFG research unit FOR-887 "Experimental Impact Cratering – The MEMIN II Program (Multidisciplinary Experimental and Modeling Impact Research Network), project KE 732/23-1 "Dynamic loading and unloading of SiO_2 aggregates. Real-time phase transformation monitored by means of synchrotron beam diffraction". Parts of this research were carried out at the light source PETRA III at DESY, a member of the Helmholtz Association (HGF). The authors also thank Prof. Dr. Falko Langenhorst for constructive discussions about the results.

References

Anderson O. L., Isaak D. G., and Yamamoto S. 1989. Anharmonicity and the equation of state for gold. *Journal of Applied Physics* 65: 1534 – 1543. Doi 10.1063/1.342969.

Birch F. 1952. Elasticity and constitution of the earth's interior. *Journal of Geophysical Research* 57: 227 – 286. Doi 10.1029/JZ057i002p00227.

Bohlen S. R. and Boettcher A. L. 1982. The quartz ↔ coesite transformation: a precise determination and the effects of other components. *Journal of Geophysical Research* 87: 7073 – 7078. Doi 10.1029/JB087iB08p07073.

Choudhury N. and Chaplot S. L. 2006. Ab initio studies of phonon softening and high-pressure phase transitions of α-quartz SiO_2. *Physical Review B* 73: 094304. Doi 10.1103/PhysRevB.73.094304.

Carl E.-R., Mansfeld U., Liermann H.-P., Danilewsky A., Langenhorst F., Ehm L., Trullenque G., Rothkirch A., and Kenkmann T. 2017: High-pressure phase transitions of α-quartz under non-hydrostatic dynamic conditions: A reconnaissance study at PETRA III. *Meteoritics & Planetary Science* (in press). Doi 10.1111/maps.12840.

Chao E. C. T., Fahey J. J., and Littler J. 1961. Coesite from Wabar Crater, near Al Hadida, Arabia. *Science* 133: 882-883. Doi 10.1126/science.133.3456.882.

Chao E. C. T., Shoemaker E. M., and Madsen B. M. 1960. 1st Natural Occurrence of Coesite. *Science* 132: 220-222. Doi 10.1126/science.132.3421.220

Chopin C. 1984. Coesite and Pure Pyrope in High-Grade Blueschists of the Western Alps - a

1st Record and Some Consequences. *Contributions to Mineralogy and Petrology* 86: 107-118. Doi 10.1007/Bf00381838.

Coes L. 1953. A new dense crystalline silica. *Science* 118: 131 – 132. Doi 10.1126/science.118.3057.131.

El Goresy A., Gillet P., Chen M., Stähle V., and Graup G. 2001. In situ finding of loci of the fabric settings of shock-induced quartz/coesite phase transition in crystalline clasts in suevite of Ries crater, Germany *Meteoritics & Planetary Science* 36: A69-A70.

Fei Y., Ricolleau A., Frank M., Mibe K., Shen G., and Prakapenka V. 2007. Toward an internally consistent pressure scale. *Proceedings of the National Academy of Sciences* 104: 9182 – 9186. Doi 10.1073/pnas.0609013104.

Ferriere L., Koeberl C., and Reimold W.U. (2009). Characterisation of ballen quartz and cristobalite in impact breccias: new observations and constraints on ballen formation. *European Journal of Mineralogy* 21: 203 – 217. Doi 10.1127/0935-1221/2009/0021-1898.

French B. M., and Koeberl C. 2010. The convincing identification of terrestrial meteorite impact structures: what works, what doesn't, and why. *Earth-Science Reviews* 98: 123 – 170. Doi 10.1016/j.earscirev.2009.10.009.

Haines J., Léger J. M., Gorelli F., and Hanfland M. 2001. Crystalline post-quartz phase in silica at high pressures. *Physical Review Letters* 87: 155503. Doi 10.1103/PhysRevLett.87.155503.

Hill R. J., Newton M. D., and Gibbs G. V. 1983. A crystal chemical study of stishovite. *Journal of Solid State Chemistry* 47: 185 – 200. Doi 10.1016/0022-4596(83)90007-5.

Huang L., Durandurdu M., and Kieffer J. 2006. Transformation pathways of silica under high pressure. *Nature Materials* 5: 977 – 981. Doi 10.1038/nmat1760.

Kingma K. J., Meade C., Hemley R. J., Mao H. K., and Veblen D.R. 1993a. Microstuctural observations of α-quartz amorphization. *Science* 259: 666 – 669. Doi 10.1126/science.259.5095.666.

Kingma K. J., Hemley R. J., Mao H. K., and Veblen D. R. 1993b. New high-pressure transformation in α-quartz. *Physical Review Letters* 70: 3927 – 3930. Doi 10.1103/PhysRevLett.70.3927.

Kirfel A., Krane H. G., Blaha P., Schwarz K., and Lippmann T. 2001. Electron-density distribution in stishovite, SiO_2: a new high-energy synchrotron-radiation study. *Acta Crystallographica section A* 57: 663-677.

Konopkova Z., Rothkirch A., Singh A. K., Speziale S., and Liermann, H. P. 2015. In situ x-ray diffraction of fast compressed iron: analysis of strains and stress under non-hydrostatic pressure. *Physical Review B* 91: 144101. Doi 10.1103/PhysRevB.91.144101.

LeBail A., Duroy H., and Fourquet J. L. 1988. Ab initio structure determination of $LiSbWO_6$ by x-ray powder diffraction. *Material Research Bulletin* 23: 447 – 452. Doi 10.1016/0025-5408(88)90019-0.

Levien L. and Prewitt C. T. 1981. High-pressure crystal structure and compressibility of coesite. *American Mineralogist* 66: 324 – 333.

Liermann H. P., Konopkova Z., Morgenroth W., Galzyrin K., Bednarcik J., McBride E. E., Petitgirard S., Delitz J. T., Wendt M., Bican Y., Ehnes A., Schwark I., Rothkirch A., Tischer M., Heuer J., Schulte-Schrepping H., Kracht T., and Franz H. 2015. The Extreme Conditions Beamline P02.2 and the Extreme Conditions Science Infrastructure at PETRA III. *Journal of Synchrotron Radiation* 22: 908 – 924. Doi 10.1107/S1600577515005937.

Martoňák R., Donadio D., Oganov A. R., and Parrinello M. 2007. From four- to six-coordinated silica: transformation pathways from metadynamics. *Physical Review B*: 76, 014120. Doi 10.1103/PhysRevB.76.014120.

McNeil L. E. and Grimsditch M. 1992. Pressure-amorphized SiO_2 α-quartz: an anisotropic amorphous solid. *Physical Review Letters* 68: 83 – 85. Doi 10.1103/PhysRevLett.68.83.

Ohtaka O., Yoshiasa A., Fukui H., Murai K. I., Oktube M., Katayama Y., Utsumi W., and Nishihata Y. 2001. Structural changes of quartz-type crystalline and vitreous GeO_2 under pressure. *Journal of Synchrotron Radiation* 8: 791 – 793. Doi 10.1107/S0909049500018306.

Perrillat J. P., Daniel I., Lardeaux J. M., and Cardon H. 2003. Kinetics of the coesite-quartz transition: application to the exhumation of ultrahigh-pressure rocks. *Journal of Petrology* 44: 773 – 788. Doi 10.1093/petrology/44.4.773.

Prescher C. and Prakapenka V. B. 2015. Dioptas: a program for reduction of two dimensional x-ray diffraction data and data exploration. *High Pressure Research* 35: 223 – 230. Doi 10.1080/08957959.2015.1059835.

Rodríguez-Carvajal J. 1993. Recent advances in magnetic structure determination by neutron powder diffraction. *Physica B* 192: 55-69.

Smyth J. R. and Hatton C. J. 1977. Coesite-Sanidine Grospydite from Roberts-Victor Kimberlite. *Earth and Planetary Science Letters* 34: 284-290. Doi 10.1016/0012-821x(77)90012-7.

Stishov S. M. and Popova S. V. 1961. A new dense modification in silica. *Geochemistry International* 10: 837-380.

Stöffler D. and Langenhorst F. 1994. Shock metamorphism of quartz in nature and experiment: I. Basic observation and theory. *Meteoritics and Planetary Science* 29: 155-181.

Teter D. M., Hemley R. J., Kresse G., and Hafner J. 1998. High pressure polymorphism in silica. *Physical Review Letters* 80: 2145 – 2148. Doi 10.1103/PhysRevLett.80.2145.

Wentzcovitch R. M., da Silva C., and Chelikowsky J. R. 1998. A new phase and pressure induced amorphization in silica. *Physical Review Letters* 80: 2149 – 2152. Doi 10.1103/PhysRevLett.80.2149.

Will G., Bellotto M., Parris W., and Hart M. 1988. Crystal structures of quartz and magnesium germinate by profile analysis of synchrotron-radiation high-resolution powder data. *Journal of Applied Crystallography* 21: 182 – 191. Doi 10.1107/S0021889887011567.

Yagi T. and Akimoto S. I. 1976. Direct determination of coesite-stishovite transition by in-situ x-ray measurements. *Tectonophysics* 35: 259 – 270. Doi 10.1016/0040-1951(76)90042-1.

Zhang J., Li B., Utsumi W., and Liebermann R.C. 1996. In situ x-ray observations of the coesite-stishovite transition: reversed phase boundary and kinetics. *Physics and Chemistry of Minerals* 23: 1 – 10.

Zinn P., Lauterjung J., and Hinze E. 1995. Kinetic studies of the crystallisation of coesite using synchrotron radiation. *Nuclear Instruments and Methods in Physics Research B* 97: 89 – 91; doi 10.1016/0168-583X(94)00348-3.